Non-culprit atherosclerotic plaque healing on serial OCT study imaging and future outcomes in patients with acute coronary syndromes

Authors:

Boling Yi [a 1], Luping He [a 1], Dirui Zhang [a 1], Ming Zeng [a], Chen Zhao [a], Wei Meng [a], Yuhan Qin [a], Ziqian Weng [a], Yishuo Xu [a], Minghao Liu [a], Xi Chen [a], Shuangtong Shao [a], Qianhui Sun [a], Wentao Wang [a], Man Li [a], Yin Lv [a], Xing Luo [a], Xiaoxuan Bai [a], Xiuzhu Weng [a], Jason L. Johnson [b], Thomas Johnson [b], Giulio Guagliumi [c], Sining Hu [a], Bo Yu [a], Haibo Jia [a]

[a] State Key Laboratory of Frigid Zone Cardiovascular Diseases (SKLFZCD), Key Laboratory of Myocardial Ischemia, Chinese Ministry of Education, Department of Cardiology of the Second Affiliated Hospital, Harbin Medical University, Harbin, Heilongjiang, China

[b] Bristol Heart Institute, Translational Health Sciences, University of Bristol, Upper Maudlin Street, Bristol, BS2 8HW, UK

[c] Division of Cardiology, IRCCS Galeazzi Sant'Ambrogio Hospital, Milan, Italy

[1] The first three authors contributed equally to this study.

Correspondence:

Sining Hu, MD, PhD

Department of Cardiology, The Second Affiliated Hospital of Harbin Medical University

National Key Laboratory of Frigid Zone Cardiovascular Diseases

The Key Laboratory of Myocardial Ischemia, Chinese Ministry of Education

246 Xuefu Road, Nangang District, Harbin 150086, China.

E-mail: hsn_831027@ 163.com

Bo Yu, MD, PhD

Department of Cardiology, The Second Affiliated Hospital of Harbin Medical University

National Key Laboratory of Frigid Zone Cardiovascular Diseases

The Key Laboratory of Myocardial Ischemia, Chinese Ministry of Education

246 Xuefu Road, Nangang District, Harbin 150086, China.

E-mail: yubodr@163.com

Abstract

Background and aims

Histologic studies indicated that healed plaque, characterized by a multilayered pattern, is indicative of prior atherothrombosis and subsequent healing. However, longitudinal in vivo data on healed plaque formation in non-culprit plaques are limited. This study aimed to investigate serial changes and clinical significance of new layered pattern formation in non-culprit plaques in patients with acute coronary syndromes (ACS) using serial optical coherence tomography (OCT) imaging.

Methods

ACS patients who underwent two OCTs at baseline and 1-year follow-up were included. Serial changes in morphologic characteristics of non-culprit plaques were evaluated. New layered pattern was defined as a new signal-rich layer on the plaque surface at follow-up that was not present at baseline.

Results

Among 553 non-culprit plaques observed in 222 patients, 82 (14.8 %) exhibited a new layered pattern at follow-up. Thin-cap fibroatheroma, macrophage, and thrombus were identified as independent predictors of the new layered pattern. Plaques with new layered pattern formation showed a greater significant reduction in luminal area and lipid content, as well as a greater increase in fibrous cap thickness compared to those without. The incidence of 6-year non-culprit-related major adverse cardiac events was higher in patients with new layered pattern than in those without (25.4 % vs. 10.8 %, $p = 0.011$), mainly due to clinically driven coronary revascularization.

Conclusions

Plaque destabilization and subsequent healing frequently occur in non-culprit plaques after ACS. The formation of a new layered pattern may contribute to temporary plaque stabilization, but results in luminal stenosis and worse clinical outcomes.

1. Introduction

Healed plaques, characterized by layers of organized thrombus or collagen, are thought to result from previous subclinical atherothrombosis and subsequent healing [1]. Autopsy studies have reported that healed plaques were common in the coronary tree of patients who died of sudden coronary death [[2], [3], [4]]. Optical coherence tomography (OCT) is capable of detecting healed plaques in vivo with high sensitivity and specificity by identifying a layered pattern, as validated in a pathology study [5]. In vivo studies have shown that healed plaques are associated with features of vascular vulnerability and that the frequency of healed plaques increases with luminal stenosis, suggesting that subclinical thrombosis and healing may play a critical role in atherosclerotic plaque progression [[6], [7], [8]]. Nevertheless, the majority of current evidence regarding healed plaque formation is derived from single-time point assessments, with a paucity of longitudinal in vivo data. A subgroup analysis of serial OCT imaging in a recent study showed that 61 % of plaques with progression had a new layered pattern [9]. However, the sample size of this study was small and did not systematically elucidate the impact of healed plaque formation on the natural history of atherosclerosis. The present serial OCT imaging study aimed to investigate serial changes and clinical significance of new layered pattern formation in non-culprit plaques in patients with acute coronary syndromes (ACS).

2. Patients and methods

2.1. Study population

Between September 2013 and December 2018, 316 patients presenting with ACS who underwent baseline and one-year (9–15 months) follow-up OCT imaging at the Second Affiliated Hospital of Harbin Medical University (Harbin, China) were included. Criteria for the diagnosis of ACS are provided in the **Supplemental Appendix**. Ninety-four patients were excluded: (1) suboptimal image quality or massive thrombus (n = 20); (2) short pullback length or imaging match length (n = 49); (3) non-culprit plaque not seen in the main epicardial vessels (n = 25). Finally, a total of 222 ACS patients with repeated OCT imaging were included in the present study, the study flowchart is shown in Supplemental Fig. S1.

This study adhered to the Declaration of Helsinki and was approved by the Ethics Committee of the Second Affiliated Hospital of Harbin Medical University, and written informed consent was obtained from all enrolled patients.

2.2. OCT imaging acquisition and analysis

OCT imaging was acquired using a commercially available C7-XR/ILUMIEN OCT system (Abbott Vascular, Santa Clara, California). All OCT images were submitted to the Intravascular Imaging and Physiology Core Lab of the Second Affiliated Hospital of Harbin Medical University and analyzed using an offline review workstation (Abbott Vascular) by two independent investigators who were blinded to patients' information. Any discordance was resolved by consensus with a third reviewer.

A non-culprit plaque was identified by OCT as a region of luminal narrowing and loss of normal vessel wall architecture (ie, intima, media, and adventitia) [10]. Two separate plaques were considered if there was a separation of at least 5 mm of normal vessels in the longitudinal view. Baseline and follow-up OCT images of target non-culprit plaques were identified by several landmarks such as side branches, calcification, coronary ostia, and stent edges. Layered pattern was defined as a plaque with one or more heterogeneous signal-rich layers of different optical intensity with clear demarcation from the underlying components and present in 3 or more consecutive frames [11]. New layered pattern was a layered pattern on the plaque surface at follow-up that was not present at baseline (Fig. 1). Quantitative and qualitative analyses of plaques were performed according to previously established criteria and consensus, and are detailed in the **Supplemental Appendix**.

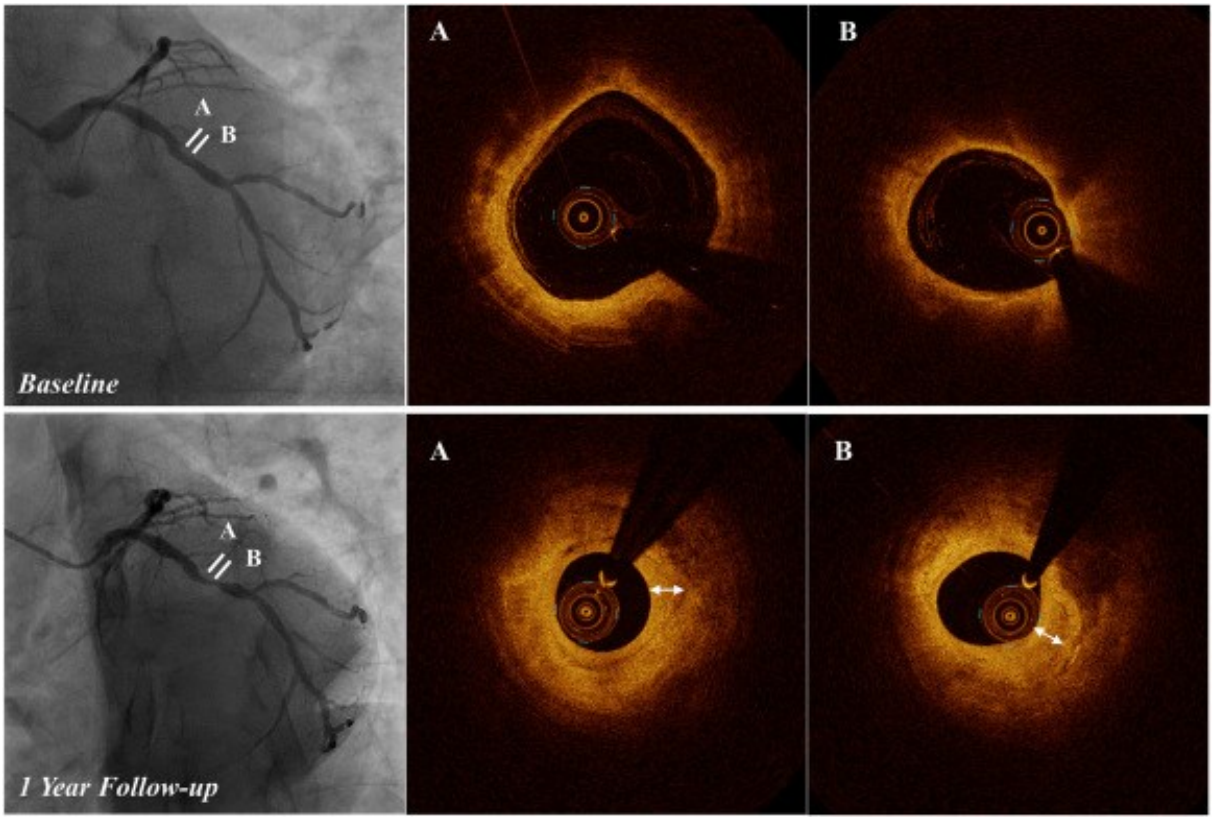

Fig. 1. Representative case of new layered pattern formation in non-culprit plaque.
At baseline, a non-culprit plaque with TCFA and macrophage accumulation (A, B) was observed in the left circumflex (MLA: 4.12 mm^2; AS%: 56.6 %). At 1-year follow-up, showed a new layered pattern (white double-headed arrows) on the surface of a fibrous plaque (C, D); and with severe progression of luminal stenosis (MLA: 1.25 mm^2; AS%: 87.1 %).
TCFA = thin-cap fibroatheroma; MLA = minimum lumen area; AS% = percent area stenosis.

2.3. Clinical follow-up

Clinical follow-up data were collected annually by dedicated clinical research coordinators via telephone calls or hospital visits after discharge. The primary endpoint was non-culprit-related major adverse cardiovascular events (MACE), including cardiac death, non-culprit-related nonfatal myocardial infarction (MI), non-culprit-related clinically driven coronary revascularization and rehospitalization for unstable or progressive angina. Cardiac death that could not be clearly related to events originating from the culprit lesion was considered to be non-culprit-related. Events that occurred prior to the follow-up OCT examination were

excluded, but events of this admission were counted. Detailed definitions of each event are presented in the **Supplemental Appendix**.

2.4. Statistical analysis

Statistical analyses were performed using SPSS version 25.0 software (IBM, Armonk, New York). Categorical data were expressed as counts (proportions). Continuous variables were tested for data distribution using the Kolmogorov-Smirnov test and expressed as mean ± SD or median (25th–75th percentiles). For patient-level data, the independent samples Student's *t*-test or the Mann-Whitney *U* test were used for continuous variables, and the chi-squared test or Fisher exact test for categorical variables. For lesion-level data, a generalized estimating equation with exchangeable correlation structure was used to account for the potential cluster effects of multiple non-culprit plaques in the same patient. Longitudinal changes within groups were compared using paired-sample t tests, Wilcoxon signed rank tests, or McNemar tests, as appropriate. To identify predictors of the new layered pattern, generalized estimating equation logistic regression was used. All the OCT plaque characteristics were tested in the univariate model and the variables with $p < 0.1$ were included in the multivariate model. The Kaplan-Meier curve was used to estimate time-to-event data. A Cox multivariable regression analysis was performed for the primary endpoint. Inter- and intra-observer agreement were assessed by κ coefficient statistics. A 2-sided *p* value of <0.05 was considered statistically significant.

3. Results

A total of 553 non-culprit plaques were identified in 222 patients with ACS who underwent serial OCT imaging. Comparing baseline and follow-up OCT images, 82 (14.8 %) plaques in 64 patients (28.8 %) developed a new layered pattern. Of these plaques, 47 (8.5 %) had a layered pattern at baseline and a new layered pattern at follow-up, while 35 (6.3 %) only had a new layered pattern at follow-up (Supplemental Fig. S2and Fig. S3).

3.1. Patient characteristics

The clinical characteristics and medications between patients with and without new layered pattern are shown in Table 1 and Supplemental Table S1. No differences were observed in OCT follow-up duration, demographics, cardiovascular risk factors, history of cardiovascular disease, clinical presentation, and medications, except that patients with new layered pattern had a higher prevalence of multivessel disease on angiogram (56.3 % vs. 41.1 %, $p = 0.041$), as well as higher fibrinogen levels and a tendency towards higher high-sensitivity C-reactive protein (hs-CRP) levels at follow-up.

Table 1. Clinical characteristics.

Empty Cell	**New Layered Pattern (+) (n = 64)**	**New Layered Pattern (−) (n = 158)**	***p*value**
Age, y	55.3 ± 10.2	54.0 ± 10.9	0.399
Males	49 (76.6)	131 (82.9)	0.274
Hypertension	36 (56.3)	73 (46.2)	0.175
Dyslipidemia	39 (60.9)	80 (50.6)	0.163
Diabetes mellitus	18(28.1)	35 (22.2)	0.344
Current smoking	38 (59.4)	99 (62.7)	0.648
Previous MI	4 (6.3)	5 (3.2)	0.496
Clinical presentation			0.874
STEMI	56 (87.5)	137 (86.7)	
NSTE-ACS	8 (12.5)	21 (13.3)	
Medication at discharge			
Aspirin	64 (100.0)	157 (99.4)	1.000
Clopidogrel	19 (29.7)	48 (30.4)	0.919
Ticagrelor	45 (70.3)	110 (69.6)	0.919

Empty Cell	**New Layered Pattern (+) (n = 64)**	**New Layered Pattern (−) (n = 158)**	***p*value**
Statin	64 (100.0)	156 (98.7)	1.000
ACEI or ARB	35 (54.7)	91 (57.6)	0.692
Laboratory data at baseline			
Total cholesterol, mg/dL	185.3 ± 39.2	180.9 ± 43.1	0.506
LDL cholesterol, mg/dL	112.8 (88.0–142.6)	110.3 (90.9–131.2)	0.851
HDL cholesterol, mg/dL	47.6 (41.3–55.7)	48.8 (40.6–58.1)	0.818
Triglyceride, mg/dL	141.3 (88.4–227.7)	129.4 (95.7–181.0)	0.434
hs-CRP, mg/L	6.0 (2.0–12.5)	5.8 (2.4–11.8)	0.821
HbA1c, %	5.8 (5.6–6.7)	5.8 (5.5–6.4)	0.841
Platelet, $*10^9$/L	225.0 (190.5–266.3)	231.5 (194.3–272.8)	0.556
Fibrinogen, mg/dL	297.5 (260.8–336.0)	280.0 (238.0–325.0)	0.183
D-dimer, ng/mL	79.5 (38.5–151.3)	76 (52.0–114.0)	0.705
LVEF, %	62.0 (58.3–63.0)	61.5 (58.0–62.0)	0.742
Laboratory data at follow-up			
Total cholesterol, mg/dL	138.4 (113.9–169.1)	131.6 (112.9–166.8)	0.459
LDL cholesterol, mg/dL	69.9 (57.3–92.3)	68.1 (55.4–96.2)	0.758
HDL cholesterol, mg/dL	47.0 (39.6–56.0)	46.1 (39.9–51.4)	0.663
Triglyceride, mg/dL	141.3 (99.5–187.8)	119.6 (86.8–180.5)	0.110
hs-CRP, mg/L	1.3 (0.8–2.7)	0.9 (0.5–2.3)	0.058
HbA1c, %	5.9 (5.6–6.7)	6.0 (5.7–6.7)	0.371

Empty Cell	**New Layered Pattern (+) (n = 64)**	**New Layered Pattern (−) (n = 158)**	***p*value**
Platelet, $*10^9$/L	226.0 (187.5–245.5)	222.0 (185.5–256.5)	0.957
Fibrinogen, mg/dL	308.5 (268.3–340.0)	283.0 (248.0–329.0)	0.025
D-dimer, ng/mL	60.5 (33.3–98.8)	53 (36.0–88.0)	0.586
LVEF, %	62.0 (60.3–63.0)	62.0 (60.0–63.0)	0.540
OCT follow-up duration, m	12.2 (12.0–12.6)	12.3 (12.0–12.5)	0.725

Values are mean ± SD, n (%), or median (25th–75th percentiles).

MI = myocardial infarction; PCI = percutaneous coronary intervention; STEMI = ST-segment elevation myocardial infarction; NSTE-ACS = non-ST segment elevation acute coronary syndrome; LDL = low-density lipoprotein; HDL = high-density lipoprotein; HbA1c = glycated hemoglobin; hs-CRP = high-sensitive C-reactive protein.

ACEI = angiotensin-converting enzyme inhibitor; ARB = angiotensin II receptor blocker.

LVEF = left ventricular ejection fraction.

3.2. Serial OCT analysis

Plaques with subsequent new layered pattern formation had a higher prevalence of lipid-rich plaque, thin-cap fibroatheroma (TCFA), macrophages, microchannels, cholesterol crystals, layered pattern, thrombus, and plaque rupture (Fig. 2), and had significantly longer lesion lengths, higher percent area stenosis, thinner fibrous cap thickness, longer lipid length, greater maximum or mean lipid arc, and higher lipid index at baseline (Supplemental Table S2). In multivariate analysis, TCFA (OR: 4.30; 95 % CI: 2.29–8.09, $p < 0.001$), macrophages (OR: 3.59; 95 % CI: 1.58–8.14, $p = 0.002$), and thrombus (OR: 5.35; 95 % CI: 2.23–12.81, $p < 0.001$) were independent OCT predictors of the new layered pattern (Supplemental Table S3).

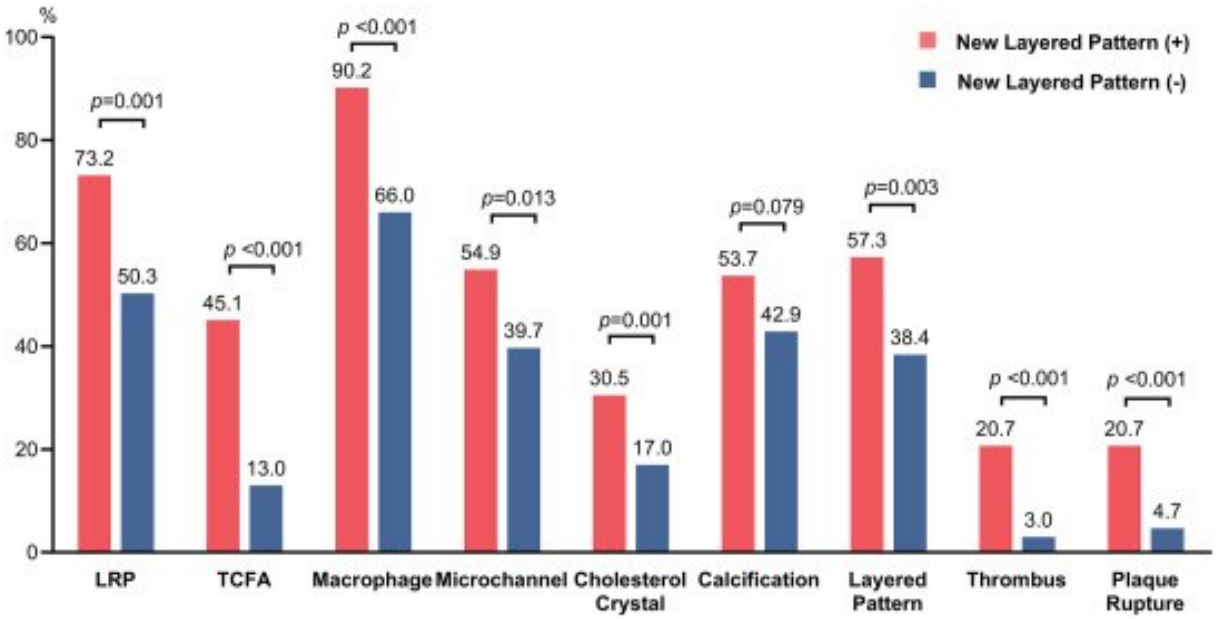

Fig. 2. Prevalence of OCT plaque characteristics between plaques with or without subsequent new layered pattern formation.

Plaques with subsequent new layered pattern formation had a higher prevalence of LRP, TCFA, macrophage, microchannel, cholesterol crystal, layered pattern, thrombus, and plaque rupture at baseline compared to those without. LRP = lipid-rich plaque; Other Abbreviations as in Fig. 1.

OCT findings at follow-up are summarized in Supplementary Table S4. During follow-up, minimum and mean lumen area significantly decreased and percent area stenosis significantly increased only in plaques with new layered pattern formation. Whereas TCFA significantly decreased, calcification significantly increased, fibrous cap thickness significantly increased, and lipid length, maximum and mean lipid arc, and lipid index significantly decreased from baseline to follow-up in 2 groups (Table 2). However, plaques that regressed to a presumably more stable type (including from TCFAs to non-TCFAs and from thick-cap fibroatheromas to non-lipid-rich plaques) were more prevalent in those with new layered pattern formation than in those without (58.3 % vs. 25.3 %, $p < 0.001$), mainly because TCFAs evolved to non-TCFAs (81.1 % vs. 47.5 %, $p = 0.001$), but not significantly from thick-cap fibroatheromas to non-lipid-rich plaques (21.7 % vs. 25.6 %, $p = 0.691$) (Fig. 3A). Consistently, the decrease in lipid length, maximum and mean lipid arc, and lipid index, and the increase in fibrous cap thickness were significantly greater in plaques with new layered pattern formation than in

those without. And for luminal stenosis, plaques with new layered plaque formation showed a greater reduction in minimum and mean lumen area, and a greater increase in percent area stenosis than those without (Fig. 3B).

Table 2. Changes in plaque characteristics between baseline and follow-up.

Empty Cell	New Layered Pattern (+) (n = 82)			New Layered Pattern (−) (n = 471)		
	Baseline	**Follow-up**	***p*value**	**Baseline**	**Follow-up**	***p*value**
Minimum lumen area, mm²	3.9 (2.6–5.9)	2.9 (2.0–5.2)	<0.001	4.0 (2.9–5.8)	4.1 (2.9–5.7)	0.121
Mean lumen area, mm²	6.2 (4.5–8.2)	5.4 (4.2–7.5)	<0.001	5.9 (4.6–7.8)	6.0 (4.5–7.7)	0.958
Area stenosis, %	52.5 (42.7–63.2)	59.0 (44.8–68.5)	<0.001	45.3 (37.3–57.1)	45.2 (34.3–55.8)	<0.001
Fibrous cap thickness, μm	60.0 (54.2–90.0)	150.0 (93.3–180.0)	<0.001[a]	106.7 (63.3–141.7)	140.0 (81.7–200.0)	<0.001[b]
Lipid length, mm	10.0 (6.2–14.0)	7.9 (5.7–12.3)	<0.001[a]	7.0 (4.8–10.5)	6.9 (4.2–9.9)	<0.001[b]
Maximum lipid arc, °	251.5 (177.8–304.1)	209 6 (141.3–267.1)	<0.001[a]	189.9 (148.9–266.7)	168.8 (141.5–250.7)	<0.001[b]
Mean lipid arc, °	171.3 (138.9–211.7)	151.2 (116.4–184.4)	<0.001[a]	148.1 (125.0–184.4)	136.8 (116.1–174.2)	<0.001[b]
Lipid index	1703.9 (993.1–2535.2)	1219.4 (753.2–2160.8)	<0.001[a]	1108.8 (691.1–1742.9)	972.5 (593.6–1531.7)	<0.001[b]

Empty Cell	New Layered Pattern (+) (n = 82)			New Layered Pattern (−) (n = 471)		
	Baseline	**Follow-up**	***p*value**	**Baseline**	**Follow-up**	***p*value**
Lipid-rich plaque	60 (73.2)	55 (67.1)	0.267	237 (50.3)	197 (41.8)	<0.001
TCFA	37 (45.1)	8 (9.8)	<0.001	61 (13.0)	36 (7.6)	<0.001
Macrophage	74 (90.2)	71 (86.6)	0.375	311 (66.0)	269 (57.1)	<0.001
Microchannel	45 (54.9)	47 (57.3)	0.727	187 (39.7)	199 (42.3)	0.162
Cholesterol crystal	25 (30.5)	29 (35.4)	0.219	80 (17.0)	87 (18.5)	0.167
Calcification	44 (53.7)	51 (62.2)	0.016	202 (42.9)	227 (48.2)	<0.001
Thrombus	17 (20.7)	8 (9.8)	0.078	14 (3.0)	3 (0.6)	0.007
Plaque rupture	17 (20.7)	14 (17.1)	0.549	22 (4.7)	21 (4.5)	1.000

Values are mean ± SD, n (%), and median (25th–75th percentiles).

TCFA = thin-cap fibroatheroma.

a

Wilcoxon signed rank test analysis was performed on 51 non-culprit plaques that were both lipid plaques at baseline and follow-up.

b

Wilcoxon signed rank test analysis was performed on 189 non-culprit plaques that were both lipid plaques at baseline and follow-up.

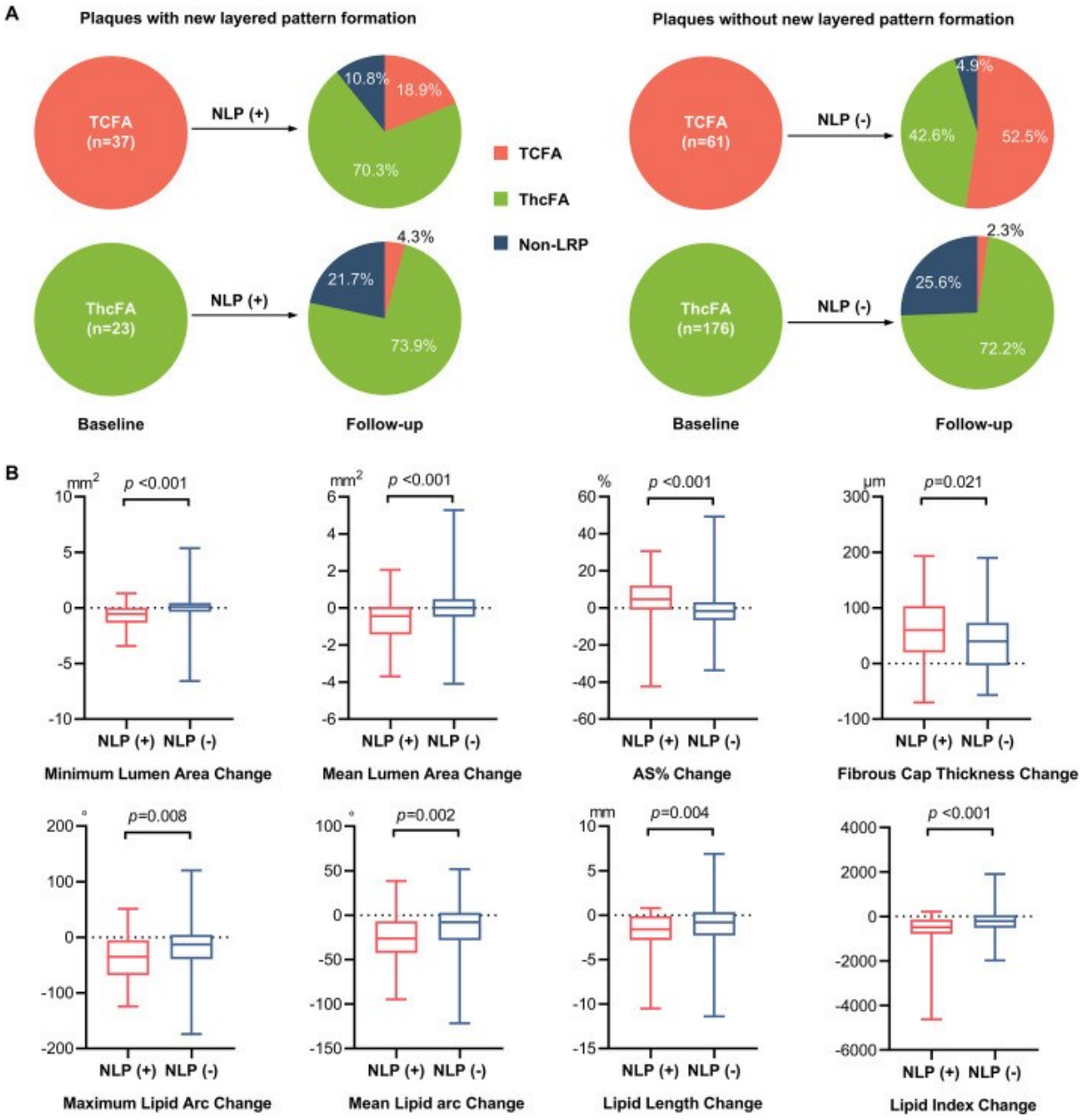

Fig. 3. Absolute Changes between plaques with or without new layered pattern formation. (A) Changes in plaque type from baseline to follow-up revealed that TCFA regression to non-TCFA was more common in those with NLP formation than in those without (p = 0.001). However, there was no significant difference in ThcFA regression to non-LRP (p = 0.691). Non-LRP includes fibrous and fibrocalcific plaques. (B) Absolute changes in lumen area, lipid content, and fibrous cap thickness revealed that the reductions in minimum and mean lumen area, lipid length, maximum and mean lipid arc, and lipid index, as well as the increases in AS% and fibrous cap thickness, were greater in plaques with NLP formation than

in those without. ThcFA = thick-cap fibroatheroma; NLP = new layered pattern; Other Abbreviations as in Fig. 1, Fig. 2.

3.3. Clinical outcomes

The median follow-up period was 73.4 months. There were 31 patients experienced the primary endpoint events (6 cardiac death, 2 non-fatal MI, 21 clinically driven coronary revascularization and 15 rehospitalization for unstable or progressive angina) during up to 6 years of follow-up. The overall 6-year cumulative patient-level non-culprit-related MACE rate was significantly higher in patients with new layered plaque formation compared to those without (25.4 % vs. 10.8 %, $p = 0.011$) (Fig. 4), and this difference was mainly driven by a higher rate of non-culprit-related coronary revascularization (18.4 % vs. 6.7 %, $p = 0.012$). Similarly, the cumulative lesion-level non-culprit-related MACE rate was also higher in the new layered pattern group (9.7 % vs. 2.4 %, $p = 0.004$) (Supplemental Table S5 and Fig. S4). After adjustment for clinical characteristics (age, sex, STEMI/NSTE-ACS at presentation, hypertension, dyslipidemia, diabetes mellitus, current smoking, previous MI), the multivariable Cox proportional hazards model revealed that patients with new layered pattern formation was positively associated with non-culprit-related MACE (hazard ratio 2.52; 95 % confidence interval 1.20–5.33, $p = 0.016$).

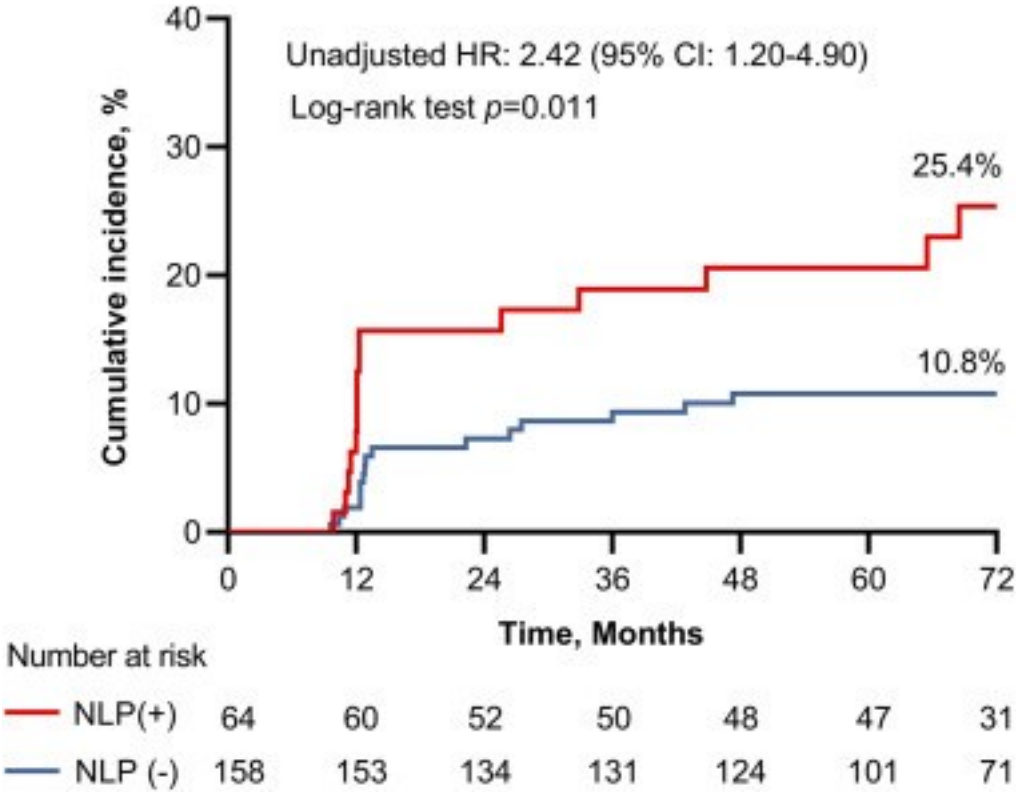

Fig. 4. Kaplan-Meier curves of non-culprit-related MACE according to patients with new layered pattern formation.

The 6-year cumulative non-culprit-related MACE was significantly higher in patients with NLP formation compared to those without. Abbreviations as in Fig. 3.

4. Discussion

The current study integrates serial in vivo OCT imaging to investigate the impact of healed plaque formation in the natural history of atherosclerosis. The main findings are as follows: (1) new layered pattern was found in more than one in seven non-culprit plaques within 1 year of follow-up after ACS, and TCFA, macrophage, and thrombus were the independent predictors; (2) layered pattern formation was associated with luminal narrowing, lipid content reduction and fibrous cap thickening; (3) layered pattern formation leads to worse clinical outcomes, primarily due to a higher incidence of non-culprit-related coronary revascularization.

Pathology and in vivo studies have shown that healed plaques are common, with prevalence in non-culprit sites ranging from 17.8 % to 46.4 % [3,[12], [13], [14]]. However, given the difficulty of observing the formation of healed plaques, current knowledge is largely derived

from single time point studies. Unexpectedly, in the present serial OCT study, up to 14.8 % of non-culprit plaques showed a new layered pattern formation after ACS. The high prevalence of new layered pattern indicates that atherosclerosis is a dynamic and discontinuous process and highlights the importance of antithrombotic therapy after ACS in promoting plaque healing to prevent occlusive thrombosis. TCFA, macrophage, and thrombus were identified as the independent predictors of the new layered pattern. TCFA is the precursor to plaque rupture and is often referred to as vulnerable plaque [2,11]. Despite considerable efforts, the positive predictive value for predicting acute events from vulnerable plaques remains low [15]. This is not attributable to a lack of plaque disruption; rather, it arises from subsequent plaque healing, which occurs when the capacity for healing is greater than the pro-thrombotic factors. Macrophage accumulation is a sign of plaque inflammatory activity and can produce matrix metalloproteinases to promote collagen breakdown, making the fibrous cap more susceptible to rupture [11]. These findings directly confirmed that the OCT-defined layered pattern is the morphologic fingerprint of previous instability and thrombosis.

The present study provides an integrated perspective and new in vivo evidence on the role of plaque healing in atherosclerosis (Fig. 5). Autopsy and in vivo studies reported that the frequency of healed plaques increased with luminal stenosis and physiological severity [7,16,17]. Previous small sample studies have reported that a proportion of plaques with progression had a new layer [9,18]. It is noteworthy that our study, which employed a large sample size, provided direct evidence that the formation of a layered pattern significantly promoted luminal stenosis. Luminal narrowing during the healing process may be caused by the accumulation of granulation tissue and smooth muscle cell proliferation, and plaque remodeling may also be involved [4,19]. Atherosclerosis has traditionally been thought of as a slow, linear growth disease [20], but our study demonstrated that rapid, stepwise progression due to repeated plaque disruption and healing is one of the major drivers of atherosclerotic progression. Interestingly, our study also found that the formation of layered pattern promoted the reduction of plaque vulnerability by decreasing in lipid content and the increasing in fibrous cap thickness. The rapid change in vulnerability may be related to lipid release and subsequent thrombus organization, as well as interstitial collagen and extracellular matrix production [1]. Nevertheless, previous OCT studies have reported that non-culprit healed

plaques have more vulnerable features [13,14]. Therefore, the stabilization of these plaques can only be considered temporary. The healing process helped avoid occlusion thrombosis, but narrowed the lumen, resulting in a "temporarily stable but narrow" healed plaque. In the absence of effective management of pro-atherosclerotic risk factors, healed plaques will continue to evolve into vulnerable plaques and enter the cycle of instability.

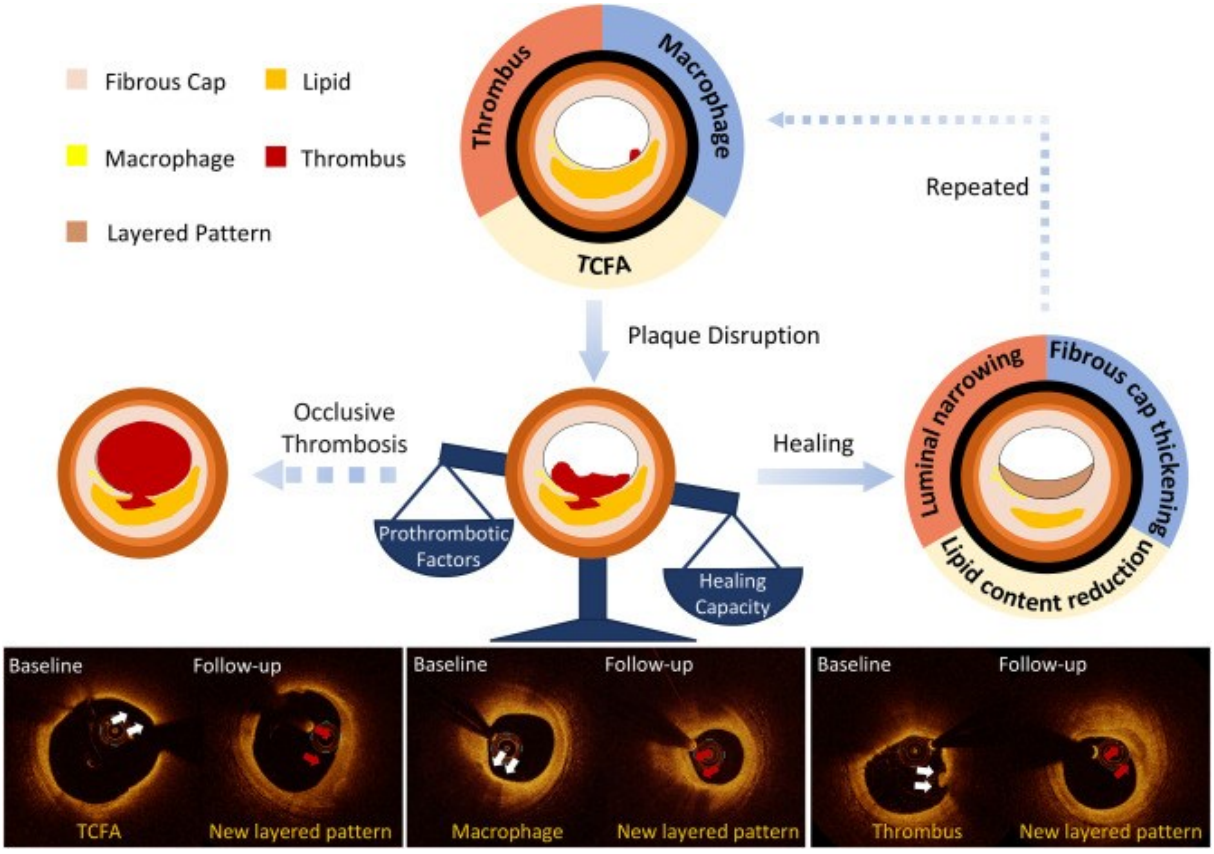

Fig. 5. Role of plaque healing in atherosclerosis.

Plaque vulnerability and thrombus are the basis for non-culprit plaque healing. After atherosclerotic plaque disruption, if the healing capacity is stronger than the prothrombotic factors, plaque will heal silently with luminal narrowing, lipid content reduction, and fibrous cap thickening; otherwise it will lead to acute occlusive thrombosis. Repeated cycles of plaque healing will lead to high-grade stenosis (Top). Representative images of plaques with TCFA or macrophage or thrombus (white arrows, respectively) at baseline and with a new layered pattern (red arrows) at follow-up (Bottom). Abbreviations as in Fig. 1. (For interpretation of the references to colour in this figure legend, the reader is referred to the Web version of this article.)

Repeated cycles of subclinical thrombosis and healing progressively reduce the luminal area, contributing to severe coronary stenosis, which not only causes chronic coronary ischemia, but may also lead to acute events triggered by small thrombi. Usui et al. [12] have reported that the presence of healed plaque itself leads to higher future non-culprit-related events. Nevertheless, our study demonstrated that healed plaque formation can be directly translated into more frequent revascularization procedures, highlighting the impact of the plaque healing process on atherosclerotic plaque progression. Further research into the mechanisms of plaque healing to balance the protective benefits and complications may help in the fight against cardiovascular disease. It is interesting to note that our study showed that LDL cholesterol had decreased to a relatively low levels at follow-up in both groups, but patients with new layered pattern had significantly higher fibrinogen levels and tended to have higher hs-CRP levels at follow-up. Fibrinogen, which is regulated by inflammatory proteins (mainly interleukin-6) and rises earlier than hs-CRP, is known to be associated with an increased risk of cardiovascular disease [21,22]. A recent meta-analysis has demonstrated that residual inflammatory risk is more strongly linked to future cardiovascular events than residual cholesterol risk [23]. These findings highlight the importance of chronic inflammation in plaque destabilization and healing, ultimately contributing to progression of atherosclerotic disease. Similarly, the prevalence of macrophages was reduced in plaques without a new layered pattern, but no significant change was observed in the new layered pattern group.

4.1. Limitations

Several limitations should be noted in this study. First, this was a single-center, retrospective, consecutive study, and the decision to perform OCT imaging was made by the operator. Therefore, there may be a selection bias. Second, three-vessel OCT imaging is not available in all patients. Third, the majority of patients in this study were treated with medication, which means that the results may not fully reflect the natural history of atherosclerosis. Fourth, plaque burden and vessel remodeling were not assessed due to the limitations of OCT imaging. Fifth, OCT-defined healed plaques were highly concordant with pathology [5], but intraplaque haemorrhages and layered patterns were difficult to distinguish on OCT imaging.

4.2. Conclusions

This serial OCT study demonstrated that new layered pattern, a sign of subclinical thrombosis and subsequent healing, occurs in up to 14.8 % of non-culprit plaques after ACS and that TCFA, macrophage, and thrombus were the independent predictors. Healed plaque formation promoted luminal narrowing, lipid content reduction, and fibrous cap thickening, and was associated with a higher risk of non-culprit-related events.

CRediT authorship contribution statement

Boling Yi: Conceptualization, Methodology, Resources, Formal analysis, Investigation, Writing – original draft, Visualization. **Luping He:** Investigation, Formal analysis. **Dirui Zhang:** Investigation, Formal analysis. **Ming Zeng:** Formal analysis, Visualization. **Chen Zhao:** Data curation. **Wei Meng:** Data curation. **Yuhan Qin:** Visualization. **Ziqian Weng:**Visualization. **Yishuo Xu:** Resources. **Minghao Liu:** Resources. **Xi Chen:** Resources. **Shuangtong Shao:** Resources. **Qianhui Sun:** Resources. **Wentao Wang:** Resources. **Man Li:** Resources. **Yin Lv:** Resources. **Xing Luo:** Resources. **Xiaoxuan Bai:** Resources. **Xiuzhu Weng:** Resources. **Jason L. Johnson:** Writing – review & editing. **Thomas Johnson:**Writing – review & editing. **Giulio Guagliumi:** Writing – review & editing. **Sining Hu:**Conceptualization, Writing – original draft, Supervision, Project administration. **Bo Yu:**Writing – review & editing, Supervision, Project administration. **Haibo Jia:** Writing – review & editing, Project administration, Funding acquisition.

Financial support

This work was supported by the Key Research and Development Program of Heilongjiang Province (2022ZX06C07), National Natural Science Foundation of China (82370464 and 82061130223) and the National Key Research and Development Program of China(2023YFC3043504).

Declaration of competing interest

The authors declare that they have no known competing financial interests or personal relationships that could have appeared to influence the work reported in this paper.

References

1. R. Vergallo, F. Crea. Atherosclerotic plaque healing. N. Engl. J. Med., 383 (2020), pp. 846-857.

2. R. Virmani, F.D. Kolodgie, A.P. Burke, A. Farb, S.M. Schwartz. Lessons from sudden coronary death: a comprehensive morphological classification scheme for atherosclerotic lesions. Arterioscler. Thromb. Vasc. Biol., 20 (2000), pp. 1262-1275.

3. J. Mann, M.J. Davies. Mechanisms of progression in native coronary artery disease: role of healed plaque disruption. Heart, 82 (1999), pp. 265-268.

4. A. Burke, F. Kolodgie, A. Farb, *et al.* Healed plaque ruptures and sudden coronary death evidence that subclinical rupture has a role in plaque progression. Circulation, 103 (2001), pp. 934-940.

5. A. Shimokado, Y. Matsuo, T. Kubo, *et al.* In vivo optical coherence tomography imaging and histopathology of healed coronary plaques. Atherosclerosis, 275 (2018), pp. 35-42.

6. F. Fracassi, F. Crea, T. Sugiyama, *et al.* Healed culprit plaques in patients with acute coronary syndromes. J. Am. Coll. Cardiol., 73 (2019), pp. 2253-2263.

7. [7]
C. Wang, S. Hu, J. Wu, *et al.* Characteristics and significance of healed plaques in patients with acute coronary syndrome and stable angina: an in vivo OCT and IVUS study. EuroIntervention, 15 (2019), pp. e771-e778.

8. J. Dai, C. Fang, S. Zhang, *et al.* Frequency, predictors, distribution, and morphological characteristics of layered culprit and nonculprit plaques of patients with acute myocardial infarction: in vivo 3-vessel optical coherence tomography study. Circ Cardiovasc Interv, 13 (2020), Article e009125.

9. M. Araki, T. Yonetsu, O. Kurihara, *et al.* Predictors of rapid plaque progression: an optical coherence tomography study. JACC Cardiovasc Imaging, 14 (2021), pp. 1628-1638.

10. S. Jiang, C. Fang, X. Xu, *et al.* Identification of high-risk coronary lesions by 3-vessel optical coherence tomography. J. Am. Coll. Cardiol., 81 (2023), pp. 1217-1230.
11. M. Araki, S.J. Park, H.L. Dauerman, *et al.* Optical coherence tomography in coronary atherosclerosis assessment and intervention. Nat. Rev. Cardiol., 19 (2022), pp. 684-703.
12. E. Usui, G.S. Mintz, T. Lee, *et al.* Prognostic impact of healed coronary plaque in non-culprit lesions assessed by optical coherence tomography. Atherosclerosis, 309 (2020), pp. 1-7.
13. M. Russo, H.O. Kim, O. Kurihara, *et al.* Characteristics of non-culprit plaques in acute coronary syndrome patients with layered culprit plaque. Eur Heart J Cardiovasc Imaging, 21 (2020), pp. 1421-1430.
14. M. Russo, F. Fracassi, O. Kurihara, *et al.* Healed plaques in patients with stable angina pectoris. Arterioscler. Thromb. Vasc. Biol., 40 (2020), pp. 1587-1597.
15. T.W. Johnson, L. Raber, C. di Mario, *et al.* Clinical use of intracoronary imaging. Part 2: acute coronary syndromes, ambiguous coronary angiography findings, and guiding interventional decision-making: an expert consensus document of the European Association of Percutaneous Cardiovascular Interventions. Eur. Heart J., 40 (2019), pp. 2566-2584.
16. Y. Matsuo, D. Higashioka, Y. Ino, *et al.* Association of hemodynamic severity with plaque vulnerability and complexity of coronary artery stenosis: a combined optical coherence tomography and fractional flow reserve study. JACC Cardiovasc Imaging, 12 (2019), pp. 1103-1105,.
17. K. Kawai, A.V. Finn, R. Virmani, C. Subclinical atherosclerosis: Part 1: what is it? Can it Be defined at the histological level? Arterioscler. Thromb. Vasc. Biol., 44 (2024), pp. 12-23.
18. M.H. Yamamoto, K. Yamashita, M. Matsumura, *et al.* Serial 3-vessel optical coherence tomography and intravascular ultrasound analysis of changing morphologies associated with lesion progression in patients with stable angina pectoris. Circ Cardiovasc Imaging, 10 (2017).
19. P. Libby. The changing landscape of atherosclerosis. Nature, 592 (2021), pp. 524-533.

20. T. Adriaenssens, M.P. Allard-Ratick, V. Thondapu, *et al.* Optical coherence tomography of coronary plaque progression and destabilization: JACC focus seminar Part 3/3. J. Am. Coll. Cardiol., 78 (2021), pp. 1275-1287.

21. S. Kaptoge, E. Di Angelantonio, L. Pennells, *et al.* C-reactive protein, fibrinogen, and cardiovascular disease prediction. N. Engl. J. Med., 367 (2012), pp. 1310-1320.

22. G. Mendieta, S. Pocock, V. Mass, *et al.* Determinants of progression and regression of subclinical atherosclerosis over 6 years. J. Am. Coll. Cardiol., 82 (2023), pp. 2069-2083.

23. P.M. Ridker, D.L. Bhatt, A.D. Pradhan, R.J. Glynn, J.G. MacFadyen, S.E. Nissen. Inflammation and cholesterol as predictors of cardiovascular events among patients receiving statin therapy: a collaborative analysis of three randomised trials. Lancet, 401 (2023), pp. 1293-1301.

Supplemental Appendix

Supplemental Methods

1. Diagnosis of acute coronary syndrome (ACS)

The diagnosis of ACS was according to the current American Heart Association (AHA)/American College of Cardiology (ACC) guidelines [1,2]. ACS included ST-segment elevation myocardial infarction (STEMI) and non-ST segment elevation acute coronary syndromes (NSTE-ACS). STEMI was defined as continuous chest pain that lasted >30 min, arrival at the hospital within 12 hours from the onset of symptoms, ST-segment elevation >0.1 mV in at least two contiguous leads or new left bundle-branch block on the 12-lead electrocardiogram, and elevated cardiac markers (creatine kinase-MB or troponin I).[1] NSTE-ACS included non–ST-segment elevation myocardial infarction (NSTEMI) and unstable angina pectoris. NSTEMI was defined as ischemic symptoms in the absence of ST-segment elevation on the electrocardiogram with elevated cardiac markers. Unstable angina pectoris was defined as having newly developed/accelerating chest symptoms on exertion or rest angina within 2 weeks without biomarker release [2].

2. Definition of cardiovascular risk factors

Hypertension was diagnosed as a documented history of systolic blood pressure ≥140 mmHg or diastolic blood pressure ≥90 mmHg or current use of antihypertensive medication. Diabetes mellitus was diagnosed if a patient met 1 of the following criteria: documented history or self-reported clinician diabetes mellitus, use of hyperglycemic medicine, fasting glucose ≥126mg/dL, 2h plasma glucose level ≥ 200mg/dL, classic symptoms with casual plasma glucose level ≥200mg/dL, or haemoglobin A1c ≥6.5%. Dyslipidemia was diagnosed as follows: with a history of hyperlipidemia, current use of drugs for dyslipidemia, total cholesterol level ≥220mg/dL, triglycerides ≥150 mg/dL, low-density lipoprotein cholesterol ≥140mg/dL, high-density lipoprotein cholesterol ≤40mg/dL. Current smoking was defined as active smoking within 1 month [3].

3. Definitions of major adverse cardiovascular events

Cardiac death was defined as death from myocardial infarction, cardiac perforation or pericardial tamponade, arrhythmia or conduction abnormalities, procedural complications, or

any death in which a cardiac cause could not be excluded. Non-fatal myocardial infarction was diagnosed by the detection of raise and fall of cardiac biomarkers (preferably troponin) above the 99th centile of the upper reference limit, together with evidence of myocardial ischemia with at least one of the following criteria: ischemic symptoms; ECG changes indicative of new ischemia (new ST-T changes or new left bundle branch block); development of pathological Q waves in the ECG; and imaging evidence of new loss of viable myocardium or new regional wall motion abnormalities. Clinically driven coronary revascularization was defined as any revascularization (percutaneous coronary intervention or coronary artery bypass graft) that is performed during follow-up that was not been planned at the index hospitalization and met ⩾ 1 of the following criteria: (1) percent diameter stenosis of ≥50% with typical ischemic symptoms, (2) percent diameter stenosis of ≥70%, (3) fractional flow reserve ≤0.80, or (4) evidence of myocardial ischemia assessed using noninvasive tests, such as nuclear imaging, and stress echocardiograph[4]. Rehospitalization for unstable or progressive angina was defined according to the Braunwald Unstable Angina Classification and the Canadian Cardiovascular Society Angina Classification. Based on angiographic data obtained at the time of the event, non-culprit–related events were adjudicated as those that occurred at initially untreated coronary segments. If the site of the event had been imaged by serial OCT, then the event was adjudicated for the lesion-level endpoint [5].

4. OCT analysis and inter- and intra-observer agreement

For each non-culprit plaque, reference lumen area was the mean of the largest lumen area proximal and distal to the stenosis. Minimum lumen area (MLA) was the smallest lumen area within the length of the plaque. Percentage of area stenosis (AS%) was calculated as ([Mean reference lumen area - MLA]/Mean reference lumen area) × 100. Lipid was defined as a signal-poor region with a diffuse border. The lipid arc was measured at 1-mm intervals, and lipid length was obtained on the longitudinal view. Lipid index was calculated as the product of mean lipid arc and lipid length. Fibrous cap thickness (FCT) was measured 3 times at the thinnest part of a lipid core and mean value was calculated [6]. Lipid rich plaque (LRP) was defined as a plaque with a maximal lipid arc >90°. Thin-cap fibroatheroma (TCFA) was defined by a maximal lipid arc >90° and thinnest FCT≤65 mm. Thick-cap fibroatheroma (ThcFA) was plaques with

maximal lipid arc >90° and thinnest FCT >65μm. Fibrocalcific plaque had evidence of calcification >90°. Fibrous plaque was defined by a homogeneous OCT signal with high backscatter and not meeting the definition of either TCFA, ThcFA, or fibrocalcific plaque.[3,6] Macrophage accumulation was identified as the presence of highly backscattering focal granular regions within the fibrous cap. Microchannel was identified as a 50-300μm signal-poor tubular structure delineated in at least 3 contiguous frames. Cholesterol crystal was present as thin and linear regions of high signal intensity with high backscattering within a plaque. Thrombus was identified as an irregular mass floating or protruding into the lumen. Calcification was identified as a signal-poor or heterogeneous area with sharp borders [6].

The inter-observer kappa coefficients for LRP, TCFA, and layered plaque were 0.88, 0.86, and 0.87, respectively. The intra-observer kappa coefficients for LRP, TCFA, and layered plaque were 0.92, 0.94 and 0.92, respectively.

Supplemental Fig. S1. Study flowchart

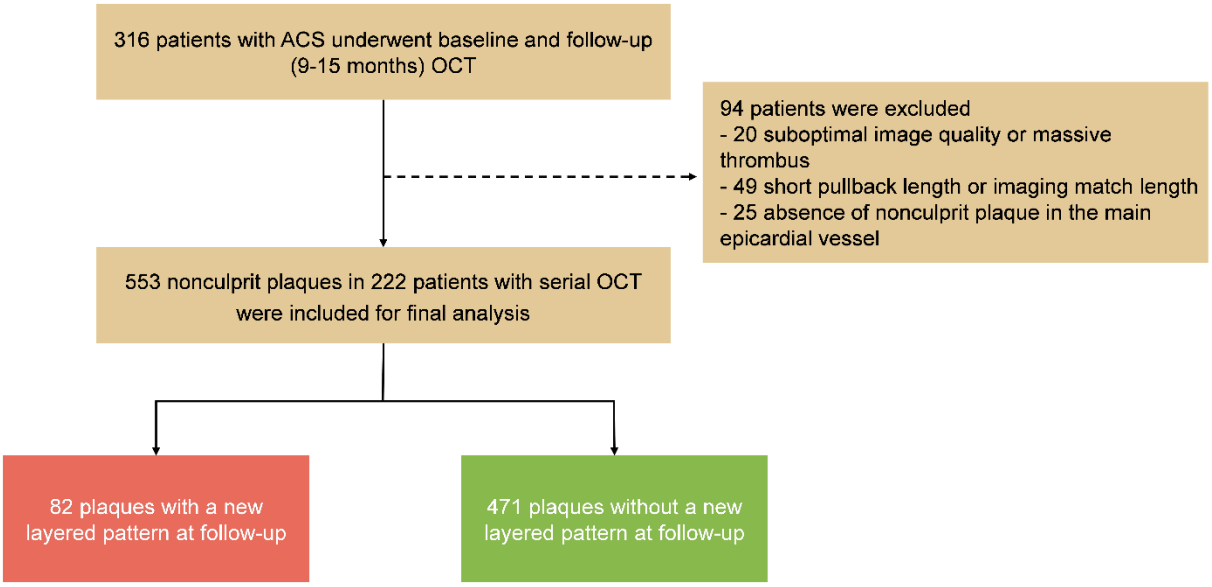

ACS = acute coronary syndrome; OCT = optical coherence tomography

Supplemental Fig. S2. Representative images of non-culprit plaques with new layered pattern formation.

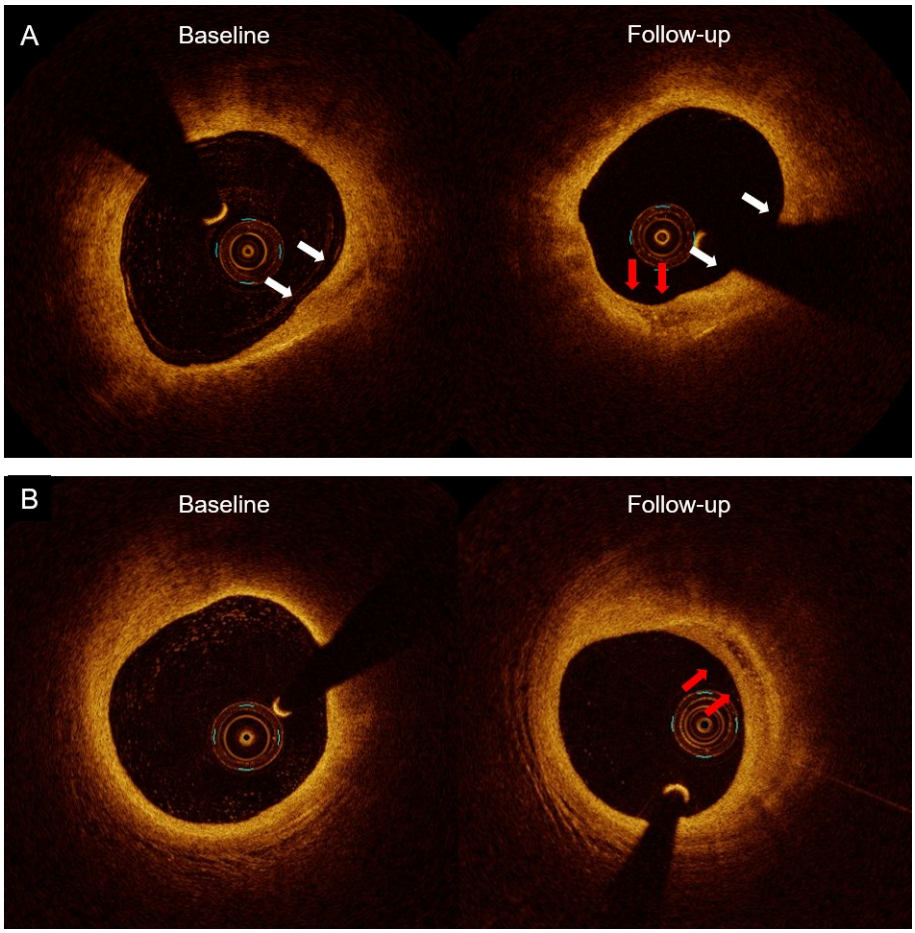

A, Representative images of plaque with a layered pattern at baseline and a new layered pattern at follow-up. B, Representative images of plaque without a layered pattern at baseline, but with a new layered pattern at follow-up. White arrow indicates a layered pattern. Red arrow indicates a new layered pattern.

Supplemental Fig. S3. Evolution of layered pattern in non-culprit plaques from baseline to follow-up.

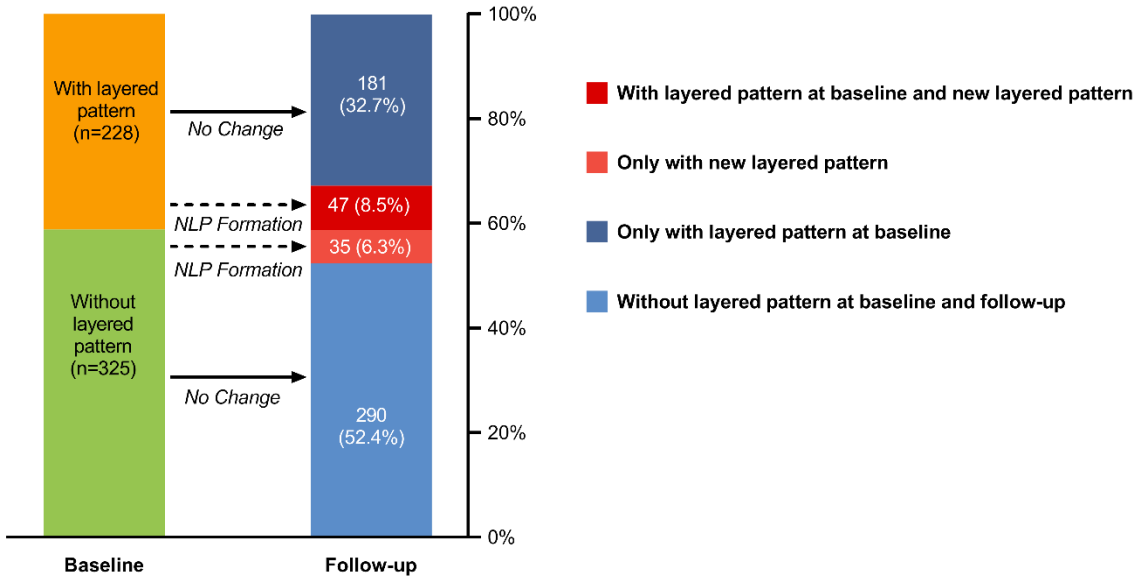

Among 553 non-culprit plaques, 82 (14.8%) plaques developed a new layered pattern, including 47 plaques had a layered pattern at baseline and a new layered pattern at follow-up, 35 plaques without a layered pattern at baseline but with a new layered pattern at follow-up. NLP = new layered pattern.

Supplemental Fig. S4. Kaplan-Meier curves of non-culprit-related MACE according to plaques with new layered pattern formation.

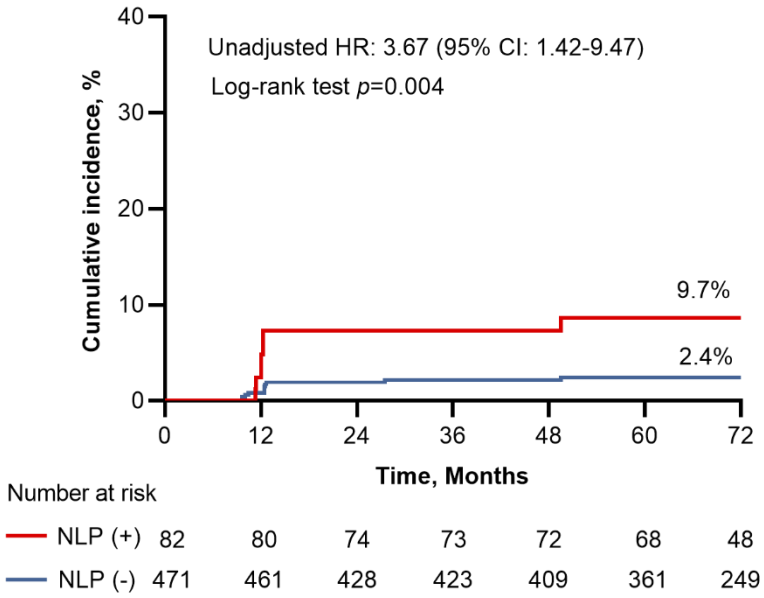

The 6-year cumulative non-culprit-related MACE was significantly higher in plaques with NLP formation compared with in those without. NLP = new layered pattern.

Supplemental Table S1. Angiography characteristics between patients with or without new layered pattern.

	New Layered Pattern (+) (n = 64)	New Layered Pattern (-) (n = 158)	*p* value
Culprit vessel			
LAD	28(43.8)	75(47.5)	0.615
LCX	8(12.5)	22(13.9)	0.779
RCA	28(43.8)	61(38.6)	0.479
TIMI flow			0.743
0/1	40(62.5)	95(60.1)	
2/3	24(37.5)	63 (39.9)	
Coronary artery disease[a]			
No significant disease	0(0)	4(2.5)	0.327
One-vessel disease	28(43.8)	89(56.3)	0.089
Two-vessel disease	23(35.9)	39(24.7)	0.090
Three-vessel disease	13(20.3)	26(16.5)	0.494
Multivessel disease	36(56.3)	65 (41.1)	0.041

Values are n (%).

[a] A significant stenosis was defined as a stenosis ≥50% of vessel diameter by visual assessment on the coronary angiogram.

LAD = left anterior descending artery; LCX = left circumflex artery; RCA = right coronary artery.

Supplemental Table S2. Baseline morphological characteristics between plaques with or without subsequent new layered pattern formation.

	New Layered Pattern (+) (n=82)	New Layered Pattern (-) (n=471)	*p* value
Location			
LAD	31(37.8)	212 (45.0)	0.239
LCX	16 (19.5)	103 (21.9)	0.693

RCA	35 (42.7)	156 (33.1)	0.127
Lesion length, mm	13.9 (10.0-18.0)	11.4 (8.6-15.5)	0.003
Minimum lumen area, mm^2	3.9 (2.6-5.9)	4.0 (2.9-5.8)	0.586
Mean lumen area, mm^2	6.2 (4.5-8.2)	5.9 (4.6-7.8)	0.088
Reference lumen area, mm^2	8.7 (6.8-10.8)	7.9 (6.3-10.1)	0.005
Area stenosis, %	52.5 (42.7-63.2)	45.3 (37.3-57.1)	0.007
Lipid-rich plaque	60 (73.2)	237 (50.3)	0.001
Fibrous cap thickness, μm	60.0 (54.2-90.0)	106.7 (63.3-141.7)	<0.001
Lipid length, mm	10.0 (6.2-14.0)	7.0 (4.8-10.5)	0.002
Maximum lipid arc, °	251.5 (177.8-304.1)	189.9 (148.9-266.7)	0.002
Mean lipid arc, °	171.3 (138.9-211.7)	148.1 (125.0-184.4)	0.002
Lipid index	1703.9 (993.1-2535.2)	1108.8 (691.1-1742.9)	<0.001
TCFA	37 (45.1)	61 (13.0)	<0.001
Macrophage	74 (90.2)	311 (66.0)	<0.001
Microchannel	45 (54.9)	187 (39.7)	0.013
Cholesterol crystal	25 (30.5)	80 (17.0)	0.001
Calcification	44 (53.7)	202 (42.9)	0.079
Layered pattern	47 (57.3)	181 (38.4)	0.003
Thrombus	17 (20.7)	14 (3.0)	<0.001
Plaque rupture	17 (20.7)	22 (4.7)	<0.001

Values are mean ± SD, n (%), or median (25th–75th percentiles).

TCFA = thin-cap fibroatheroma; LAD = left anterior descending artery; LCX = left circumflex artery; RCA = right coronary artery

Supplemental Table S3. OCT predictors of the new layered pattern.

	Univariable			Multivariable		
	Odds Ratio	95% CI	p value	Odds Ratio	95% CI	*p* value
LRP						
ThcFA	0.63	0.35-1.12	0.117			
TCFA	5.63	3.25-9.74	<0.001	4.30	2.29-8.09	<0.001
Macrophage	4.53	2.27-9.02	<0.001	3.59	1.58-8.14	0.002
Microchannel	1.78	1.13-2.82	0.013	1.13	0.66-1.93	0.647
Cholesterol crystal	2.34	1.39-3.95	0.001	0.88	0.48-1.61	0.668
Layered pattern	2.00	1.26-3.19	0.003	1.14	0.67-1.92	0.628
Calcification	1.51	0.95-2.40	0.079	0.91	0.52-1.57	0.727
Thrombus	8.56	4.02-18.22	<0.001	5.35	2.23-12.81	<0.001
plaque rupture	5.85	3.06-11.21	<0.001	1.24	0.51-3.04	0.640

CI = confidence interval; LRP = lipid-rich plaque; TCFA = thin-cap fibroatheroma; ThcFA = thick-cap fibroatheroma.

Supplemental Table S4. Follow-up morphological characteristics between plaques with or without a new layered pattern.

	New Layered Pattern (+) (n=82)	New Layered Pattern (-) (n=471)	*p* value
Lesion length, mm	13.8 (10.5-19.7)	11.3 (8.5-15.2)	<0.001
Minimum lumen area, mm^2	2.9 (2.0-5.2)	4.1 (2.9-5.7)	0.084
Mean lumen area, mm^2	5.4 (4.2-7.5)	6.0 (4.5-7.7)	0.651
Area stenosis, %	59.0 (44.8-68.5)	45.2 (34.3-55.8)	<0.001
Lipid-rich plaque	55 (67.1)	197 (41.8)	<0.001
Fibrous cap thickness, μm	150.0 (93.3-180.0)	140.0 (81.7-200.0)	0.501
Lipid length, mm	7.9 (5.7-12.3)	6.9 (4.2-9.9)	0.089
Maximum lipid arc, °	209 6 (141.3-267.1)	168.8 (141.5-250.7)	0.297
Mean lipid arc, °	151.2 (116.4-184.4)	136.8 (116.1-174.2)	0.473
Lipid index	1219.4 (753.2-2160.8)	972.5 (593.6-1531.7)	0.094
TCFA	8 (9.8)	36 (7.6)	0.647
Macrophage	71 (86.6)	269 (57.1)	<0.001
Microchannel	47 (57.3)	199 (42.3)	0.014
Cholesterol crystal	29 (35.4)	87 (18.5)	<0.001
Calcification	51 (62.2)	227 (48.2)	0.030
Layered pattern	82 (100.0)	181 (38.4)	0.009
Thrombus	8 (9.8)	3 (0.6)	<0.001
Plaque rupture	14 (17.1)	21 (4.5)	<0.001

Values are mean ± SD, median (25th–75th percentiles), or n (%).

TCFA = thin-cap fibroatheroma.

Supplemental Table S5. Kaplan-Meier estimates for cumulative rates of clinical events at 6 years.

	New Layered Pattern (+)	New Layered Pattern (-)	*p* value
Patient-level	n=64	n=158	
NC-related MACE	25.4 (15)	10.8 (16)	0.011
Cardiac death	5.8 (3)	2.1 (3)	0.306
NC-related MI	0	1.3 (2)	0.362
NC-related coronary revascularization	18.4 (11)	6.7 (10)	0.012
NC-related Rehospitalization for unstable or progressive angina	11.1 (7)	5.5(8)	0.124
Lesion-level	n=82	n=471	
NC-related MACE	9.7 (7)	2.4 (11)	0.004
NC-related MI	0	0.2 (1)	0.670
NC-related coronary revascularization	8.7 (7)	1.8 (9)	0.001
NC-related Rehospitalization for unstable or progressive angina	2.4 (2)	0.9 (4)	0.208

Values are % (n).

NC= non-culprit; MACE = major adverse cardiac events; MI = myocardial infarction.

Reference

1. O'Gara PT, Kushner FG, Ascheim DD et al. 2013 ACCF/AHA guideline for the management of ST-elevation myocardial infarction: a report of the American College of Cardiology Foundation/American Heart Association Task Force on Practice Guidelines. J Am Coll Cardiol 2013;61:e78-e140.
2. Amsterdam EA, Wenger NK, Brindis RG et al. 2014 AHA/ACC guideline for the management of patients with non-ST-elevation acute coronary syndromes: a report of the American College of Cardiology/American Heart Association Task Force on Practice Guidelines. Circulation 2014;130:e344-426.
3. Cao M, Zhao L, Ren X et al. Pancoronary Plaque Characteristics in STEMI Caused by Culprit Plaque Erosion Versus Rupture: 3-Vessel OCT Study. JACC Cardiovasc Imaging 2021;14:1235-1245.
4. HM G-G, EP M, A F et al. Standardized End Point Definitions for Coronary Intervention Trials: The Academic Research Consortium-2 Consensus Document. Circulation 2018;137:2635-2650.
5. Jiang S, Fang C, Xu X et al. Identification of High-Risk Coronary Lesions by 3-Vessel Optical Coherence Tomography. J Am Coll Cardiol 2023.
6. Tearney GJ, Regar E, Akasaka T et al. Consensus standards for acquisition, measurement, and reporting of intravascular optical coherence tomography studies: a report from the International Working Group for Intravascular Optical Coherence Tomography Standardization and Validation. J Am Coll Cardiol 2012;59:1058-72.